Non-degenerate Priors for Arbitrarily Deep Networks

David Duvenaud
University of Cambridge
dkd23@cam.ac.uk

Oren Rippel
Harvard University
rippel@math.mit.edu

Ryan Adams
Harvard University
rpa@seas.harvard.edu

Zoubin Ghahramani
University of Cambridge
zoubin@eng.cam.ac.uk

Abstract

Choosing approrpriate architectures and initialization strategies are crucial to good performance of deep networks. To shed light on this problem, we analyze the analogous problem of constructing useful priors on deep functions. We show that for typical deep architectures, the representational capacity of the network tends to capture fewer degrees of freedom as the number of layers increases, retaining only a single degree of freedom in the limit. We propose alternate priors on network structure which do not suffer from these pathologies. We also derive novel kernels obtained by composing infinitely-many feature transforms.

1 Introduction

Much recent work on deep learning has focused on weight initialization

Deep Gaussian processes are a prior on functions of the form: $f_{deep} = f^{1:L}(\mathbf{x}) = f^L(f^{L-1}(\dots f^3(f^2(f^1(\mathbf{x})))\dots))$, where each $f \overset{\text{iid}}{\sim} \text{GP}$.

2 The relation between deep nets and deep Gaussian processes

2.1 A neural net with one hidden layer

In a neural net with a single hidden layer, the correspondence is simple: The features $\phi(\mathbf{x})$ correspond to the hidden units. In the typical definition of a multi-layer perception, the hidden units of the first layer are defined as:

$$\Phi(\mathbf{x}) = h^{(1)}(\mathbf{x}) = \sigma(b^{(1)} + W^{(1)}\mathbf{x}) \tag{1}$$

The output $f(\mathbf{x})$ is simply a weighted sum of these hidden unit activations, for both GP models and neural networks.

[9] showed that Gaussian process priors can be viewed as the limiting distribution of a neural network with infinitely many hidden units. More precisely, he showed that for models of the form

$$f(x) = \alpha^T \Phi(x) = \sum_{i=i}^{K} \alpha_i \phi_i(x), \tag{2}$$

the central limit theorem implies that any two function values $f(x), f(x')$ have a joint distribution approaching a Gaussian as $K \to \infty$ with fixed feature vector $\Phi(x)$ and i.i.d. α. The result is

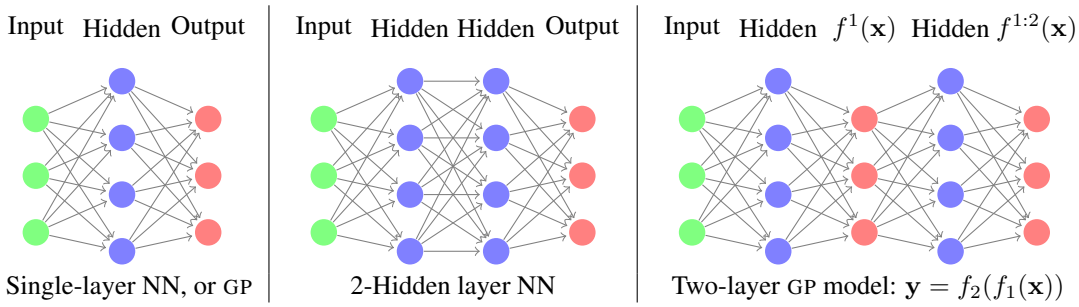

Figure 1: Comparing architectures. When there are multiple layers, there are two possible meanings of "hidden units" in the deep GP model. We can either consider every second layer to be a linear combination of an infinite number of parametric hidden basis functions, or we can integrate out the hidden layers, and consider the deep GP to be a neural network with a finite number of hidden units, each with a different non-parametric activation function.

surprisingly general: It doesn't put any constraints on what the features are (other than having bounded activation), nor does it require that the feature weighs α be Gaussian distributed. It only requires that the distribution on weights α has finite variance, and that as we increase the number of features K, we divide the feature weights by K. As $K \to \infty$, the central limit theorem gives that the weighted sum of feature activations approaches a Gaussian distribution.

2.2 A neural net with two hidden layers

In a neural net with two hidden layers, the correspondence is a little more complicated. Generally, the n^{th} layer units are given be the recurrence:

$$h^{(n)}(\mathbf{x}) = \sigma(b^{(n)} + W^{(n)} h^{(n-1)}(\mathbf{x})) \tag{3}$$

for real-valued outputs, the function can be written as weighted sum of the last layer's hidden units:

$$f(\mathbf{x}) = W^{(top)} \sigma(b^{(n)} + W^{(n)} h^{(n-1)}(\mathbf{x})) = W^{(top)} h^{(n)}(\mathbf{x})) \tag{4}$$

We can also write deep GP models in this way. However, for many covariance functions, we can't explicitly compute the activation of infinitly-many hidden functions $\Phi(\mathbf{x})$, and instead can only examine their weighted sum. Hence, to be able to compare the two model classes, we will view deep GP models in a different way, as a neural network with a finite number of nonparametric basis functions, where the outputs of $f^{1:\ell}(\mathbf{x})$ represent the output of the hidden nodes at the $\ell^{th} layer$.

Figure 1 compares these two architectures. If we stick to the correspondence between neural nets and GPs as defined in (2), we notice that the deep GP architecture forces the linear connections between hidden layers go be squeezed through a finite set of nodes, corresponding to the output of the independent GPs at each layer. However, there is another interpretation of this architecture. We can integrate out the hidden layers, and consider the deep GP to be a neural network with a finite number of hidden units, each with a different non-parametric activation function. Using this second view lets us compare GP models to multilayer perceptrons more directly, examining the activations and shapes of the finite number of basis functions at each layer.

2.3 The relation between initialization strategies, regularization, and priors

Traditional training of deep networks requires both an an initialization strategy, and a regularization method. In a Bayesian model, the prior implicitly defines both of these things.

The effects of automatic relevance determination One feature of Gaussian process models that doesn't have a clear anologue in the neural-net literature is automatic relevance determination (ARD). Recall that in the ARD procedure, the lengthscales of each dimension are scaled to maximize the marginal likelihood of the GP. In standard one-layer GP regression, it has the effect of smoothing out the posterior over functions in directions in which the data does not change.

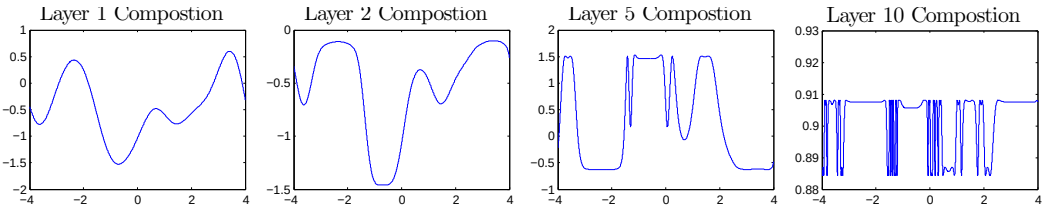

Figure 2: One-dimensional draws from a deep GP prior. After a few layers, the functions begin to be either nearly flat, or highly varying, everywhere. This is a consequence of the distribution on derivatives becoming heavy-tailed.

Sparse Initialization [7] used sparse initialization, in which each hidden unit had 15 non-zero incoming connections. While it is not clear if deep GPs have analogous problems with saturation of connection weights, we note that an anologous initialization strategy would be to put a heavy-tailed prior on the lengthscales in the squared-exp kernel.

3 One-dimensional Asymptotics

First, we derive the limiting distribution for the derivative of a one-dimensional deep GP. The derivative of a one-dimensional deep GP is simply a product of i.i.d Normal R.V.'s, with zero mean and variance σ_f^2/ℓ^2. The distribution of the absolute value of the derivative of the deep function is a product of half-normals:

$$\frac{\partial f(x)}{\partial x} \overset{iid}{\sim} \mathcal{N}\left(0, \frac{\sigma_f^2}{\ell^2}\right) \implies \left|\frac{\partial f(x)}{\partial x}\right| \overset{iid}{\sim} \text{half}\mathcal{N}\left(\sqrt{\frac{2\sigma_f^2}{\pi\ell^2}}, \frac{\sigma_f^2}{\ell^2}\left(1-\frac{2}{\pi}\right)\right) \tag{5}$$

Thus if $\sigma_f^2/\ell_{d_1}^2 = \pi/2$, then $\mathbb{E}\left[\left|\partial f(x)/\partial x\right|\right] = 1$, and so $\mathbb{E}\left[\left|\partial f^{1:L}(x)/\partial x\right|\right] = 1$. If σ_f^2/ℓ^2 is less than $\pi/2$, the expected derivative magnitude goes to zero, and if it's greater, then the expected magnitude goes to infinity.

The log of this variable has moments:

$$m_{\log} = \mathbb{E}\left[\log\left|\frac{\partial f(x)}{\partial x}\right|\right] = 2\log\left(\frac{\sigma_f}{\ell}\right) - \log 2 - \gamma \tag{6}$$

$$v_{\log} = \mathbb{V}\left[\log\left|\frac{\partial f(x)}{\partial x}\right|\right] = \frac{\pi^2}{4} + \frac{\log^2 2}{2} - \gamma^2 - \gamma\log 4 + 2\log\left(\frac{\sigma_f}{\ell}\right)\left[\gamma + \log 2 - \log\left(\frac{\sigma_f}{\ell}\right)\right]$$

where $\gamma \approxeq 0.5772$ is Euler's constant. Since the second moment is finite, by the central limit theorem, the limiting distribution of the size of the gradient is log-normal:

$$\log\left|\frac{\partial f^{1:L}(x)}{\partial x}\right| = \sum_{i=1}^{L}\log\left|\frac{\partial f^{L}(x)}{\partial x}\right| \implies \log\left|\frac{\partial f^{1:L}(x)}{\partial x}\right| \overset{L\to\infty}{\sim} \mathcal{N}\left(Lm_{\log}, L^2 v_{\log}\right) \tag{7}$$

Even if the expected magnitude of the derivative remains constant, the variance of the distribution grows without bound, and so will almost surely be very small almost everywhere, with rare but very large jumps.

With high probability, the regions of $f^{1:L}(\mathbf{x})$ which vary quickly will be the same regions in which $f^{1:L+1}(\mathbf{x})$ has high variance.

Figure 2 shows draws from a 1D deep GP prior at varying depths.

4 The Jacobian of Deep GPs is a product of i.i.d. Normal Matrices

In this section, we show a result which will let us characterize the Jacobians of arbitrarily deep networks drawn from a deep GP prior.

Lemma 4.1. *The partial derivatives of a function drawn from a* GP *prior with a product kernel are i.i.d. Gaussian distributed.*

Proof. Because differentiation is a linear operator, the derivatives of a function drawn from a GP prior are also jointly Gaussian distributed. The covariance between partial derivatives w.r.t. input dimensions d_1 and d_2 of vector $\mathbf{x}$ are given by [16]:

$$\operatorname{cov}\left(\frac{\partial f(\mathbf{x})}{\partial x_{d_1}}, \frac{\partial f(\mathbf{x})}{\partial x_{d_2}}\right) = \left.\frac{\partial^2 k(\mathbf{x}, \mathbf{x}')}{\partial x_{d_1} \partial x'_{d_2}}\right|_{\mathbf{x}=\mathbf{x}'} \tag{8}$$

If our kernel is a product over individual dimensions $k(\mathbf{x}, \mathbf{x}') = \prod_d^D k_d(x_d, x'_d)$, as in the case of the isotropic squared-exp kernel, then the off-diagonal entries are zero, implying that all elements are independent and identically distributed. □

In the case of the isotropic squared-exp kernel, the covariance between derivatives has the form:

$$k_{SE}(\mathbf{x}, \mathbf{x}') = \sigma_f^2 \prod_{d=1}^{D} \left(-\frac{1}{2}\frac{(x_d - x'_d)^2}{\ell_d^2}\right) \implies \operatorname{cov}\left(\frac{\partial f(\mathbf{x})}{\partial x_{d_1}}, \frac{\partial f(\mathbf{x})}{\partial x_{d_2}}\right) = \begin{cases} \frac{\sigma_f^2}{\ell_{d_1}^2} & \text{if } d_1 = d_2 \\ 0 & \text{if } d_1 \neq d_2 \end{cases} \tag{9}$$

Lemma 4.2. *The Jacobian of a* GP *with a seperable kernel is a matrix of i.i.d. Gaussian R.V.'s*

Proof. The Jacobian of the vector-valued function $f(\mathbf{x})$ is a matrix J whose i, j^th element is $J_{ij} = \frac{\partial f_i(\mathbf{x})}{\partial x_j}$. When composing L different functions, we'll denote the *immediate* Jacobian of the function mapping from layer $\ell - 1$ to layer ℓ as $J^\ell(\mathbf{x})$, and the Jacobian of the entire composition of L functions by $J^{1:L}(\mathbf{x})$.

Because we've assumed that the GP on each output dimension $f_d(\mathbf{x}) \sim \mathcal{GP}$ is independent, it follows that for a given $\mathbf{x}$, each row of $J_{\mathbf{x}\to\mathbf{y}}(\mathbf{x})$ is independent. Above, we showed that the elements of each row are independent. This means that each entry in the Jacobian of a GP-distributed transform is i.i.d. Normal. □

Theorem 4.3. *The Jacobian of a deep* GP *using a product kernel is a product of indepedent random Gaussian matrices.*

Proof. By the multivariate chain rule, the Jacobian of a composition of functions is simply the product of the Jacobian matrices of each function. Thus the Jacobian of the composed (deep) function $f^L(f^{L-1}(\dots f^3(f^2(f^1(\mathbf{x})))\dots))$ is:

$$J^{1:L}(x) = J^L J^{L-1} \dots J^3 J^2 J^1 \tag{10}$$

Since each $J_{i,j}^\ell \overset{\text{iid}}{\sim} \mathcal{N}\left(0, \frac{\sigma_f^2}{\ell^2}\right)$, the complete Jacobian is a product of i.i.d. Gaussian matrices. □

Theorem 4.3 allows us to analyze the representational properties of a deep Gaussian process by simply examining the properties of products of i.i.d. Gaussian matrices.

5 Formalizing the pathology

5.1 Jacobian Singular Value Spectrum

[12] argue that a good latent representation is invariant in directions orthogonal to the manifold on which the data lie. Conversely, a good latent representation must also change in directions tangent to the data manifold, in order to preserve relevant information. Figure 3 visualizes this idea. We follow [13] in characterizing the representational properties of a function by the singular value spectrum of the Jacobian[1].

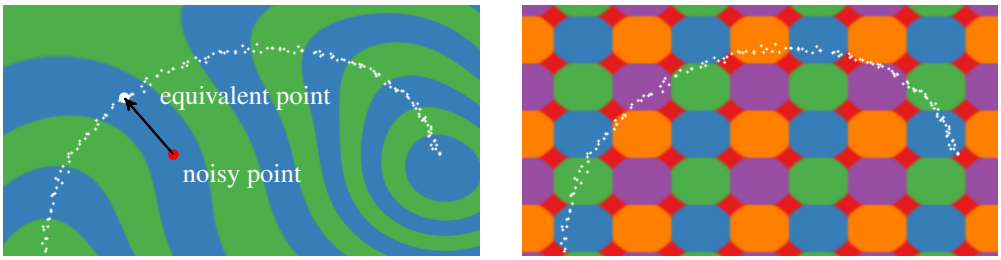

A compact, noise-tolerant latent representation of a one-dimensional manifold

A naïve latent representation of a one-dimensional manifold

Figure 3: Comparing different latent representations of data on a 1-D manifold. A good latent representation is invariant in directions orthogonal to the data manifold, making the representation robust to noise in those directions. The representation must also change in directions tangent to the manifold, in order to preserve information for later layers.

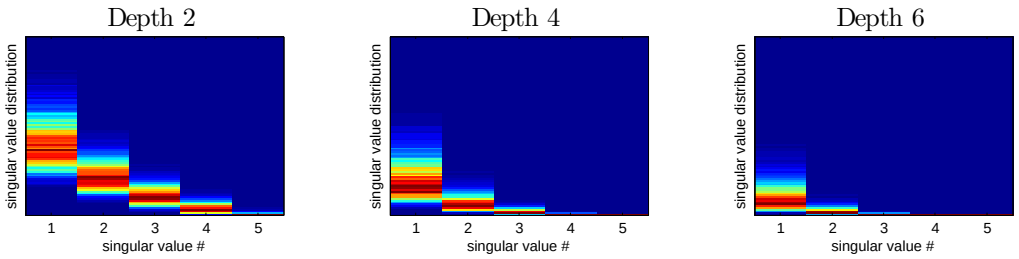

Figure 4: Singular value spectrum of the Jacobian of a deep GP. As the net gets deeper, the largest singular value dominates. This implies that there is only one effective degree of freedom in the representation being computed.

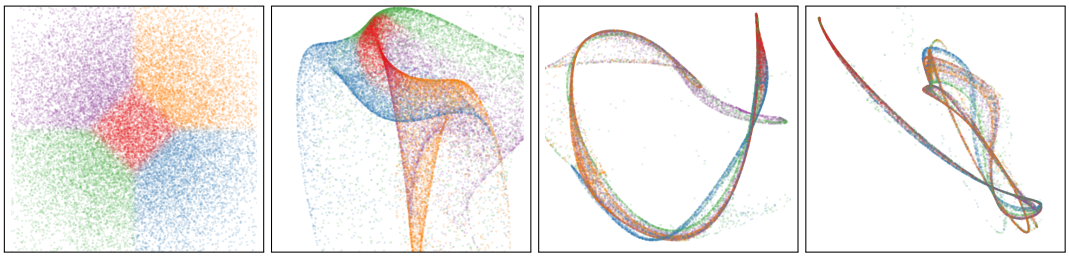

$p(\mathbf{x})$ $p(f^1(\mathbf{x}))$ $p(f^{1:4}(\mathbf{x}))$ $p(f^{1:6}(\mathbf{x}))$

Figure 5: Draws from a deep GP. A distribution is warped by successive functions drawn from a GP prior. As the number of layers increases, the density exhibits a sort of filamentation.

Figure 4 shows the spectrum for deep GPs of different depths. As the net gets deeper, the largest singular value dominates. This implies that there is only one effective degree of freedom in representation being computed. As well, the distribution on singular vlaues becomes heavy-tailed.

Figure 5 demonstrates a related pathology that arises when composing functions to produce a deep latent-variable model. The density in observed space eventually becomes locally concentrated onto one-dimensional manifolds, or *filaments*.

To visualize this pathology in another way, figure 6 illustrates the value that at each point in the input space is mapped to, after successive warpings. After 40 warpings, we can see that locally, there is usually only one direction that one can move in $\mathbf{x}$-space in order to change the value of the function.

[1] [13] examine the Jacobian at the training points, but the models we are examining are stationary, so it doesn't matter where we examine the function.

Identity Map: $\mathbf{y} = \mathbf{x}$ | 1 Layer: $\mathbf{y} = f^1(\mathbf{x})$ | 2 Layers: $\mathbf{y} = f^{1:2}(\mathbf{x})$ | 40 Layers

Figure 6: Feature Mapping of a deep GP. Shown here are the colors corresponding to the location $\mathbf{y} = f(\mathbf{x})$ that each point is mapped to after being warped by a deep GP. Just as the densities in 5 became locally one-dimensional, there is locally only one direction that one can move $\mathbf{x}$ in to change $\mathbf{y}$. Regions where the colors change rapidly indicate that the Jacobian is large in that area.

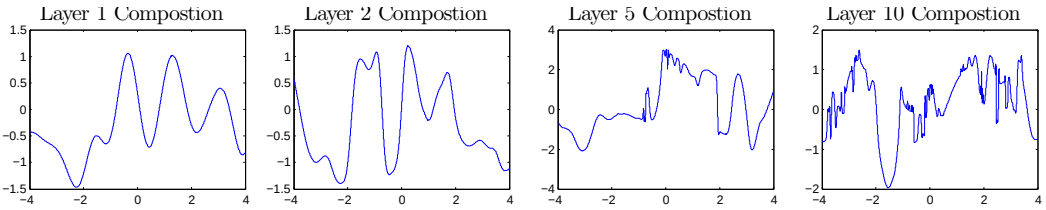

Figure 7: One-dimensional draws from a deep GP prior with eeach layer connected to the input. Even after many layers, the functions remain smooth in some regions, while varying rapidly in other regions.

To what extent are these pathologies present in nets being used today? In simulations, we found that for deep functions with a fixed latent dimension D, the singular value spectrum remained relatively flat for hundreds of layers as long as $D > 100$. Thus, these pathologies are unlikely

5.2 Fixing the pathology

Follow a suggestion from [9], we can fix the pathologies exhibited in figures 5 and 6 by simply making each layer of computation depend not only on the output of the previous layer, but also on the original input $\mathbf{x}$. Draws from the resulting priors are shown in figures 8 and 9. Figure 7 shows draws from a 1D deep GP prior with a connected architecture.

Jacobians of connected deep networks We can similarily examine the Jacobians of the new connected architecture. The Jacobian of a composite function which has had the original inputs

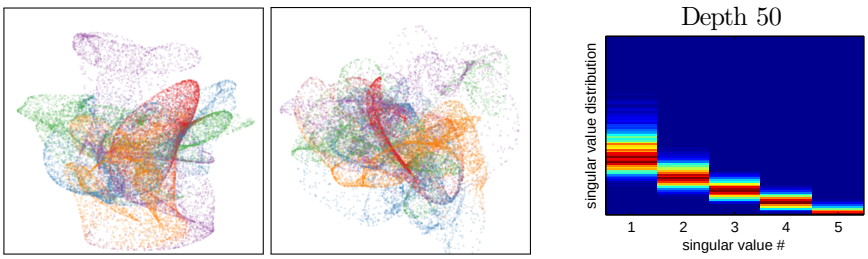

4 Layers | 5 Layers | Singular Value Spectrum

Figure 8: Left: Densities defined by a draw from a deep GP, with each layer connected to the input $\mathbf{x}$. As depth increases, the density becomes more complex without concentrating along filaments. Right: The singular value spectrum of a 6-dimensional deep GP prior 50 layers deep. The singular values remain roughly the same scale.

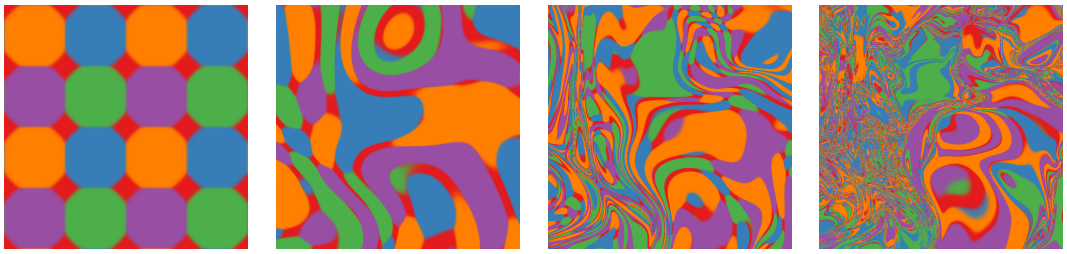

Identity Map: $\mathbf{y} = \mathbf{x}$ | 2 connected Layers | 10 Connected Layers | 40 Connected Layers

Figure 9: Feature Mapping of a deep GP with each layer connected to the input $\mathbf{x}$. Just as the densities in 8 became remain locally two-dimensional even after many transformations, in this mapping there are locally usually two directions that one can move in $\mathbf{x}$ to change $\mathbf{y}$.

appended $f_{\text{aug}}(\mathbf{x}) = [f(\mathbf{x}), \mathbf{x}]$, is $\begin{bmatrix} J_f \\ I_D \end{bmatrix}$ and the Jacobian of all one-layer transformations of these augmented functions are $D \times 2D$ matrices. The Jacobian of the composed, connected deep function is defined by the recurrence: $J^{1:L}(\mathbf{x}) = J^L \begin{bmatrix} J^{1:L-1} \\ I_D \end{bmatrix}$

6 Arbitarily Deep Kernels

[3] investigated kernels constructed by applying multiple layers of feature mappings. That is to say, if a kernel has the form $k_1(\mathbf{x}, \mathbf{x}') = \Phi(\mathbf{x})^\mathsf{T}\Phi(\mathbf{x})$, then we can consider constructing a kernel based on the repeated feature mapping: $k_2(\mathbf{x}, \mathbf{x}') = k_2(\Phi(\mathbf{x}), \Phi(\mathbf{x}')) = \Phi(\Phi(\mathbf{x}))^\mathsf{T}\Phi(\Phi(\mathbf{x}))$.

For the squared-exp kernel, this composition operation has a closed form:

$$k_{n+1}(\mathbf{x}, \mathbf{x}') = \exp\left(-\frac{1}{2}||\Phi_n(\mathbf{x}) - \Phi_n(\mathbf{x}')||_2^2\right) \tag{11}$$

$$k_{n+1}(\mathbf{x}, \mathbf{x}') = \exp\left(-\frac{1}{2}\sum_i \left[\phi_n^{(i)}(\mathbf{x}) - \phi_n^{(i)}(\mathbf{x}')\right]^2\right) \tag{12}$$

$$k_{n+1}(\mathbf{x}, \mathbf{x}') = \exp\left(-\frac{1}{2}\left[k_n(\mathbf{x}, \mathbf{x}) - 2k_n(\mathbf{x}, \mathbf{x}') + k_n(\mathbf{x}', \mathbf{x}')\right]\right) \tag{13}$$

$$k_{n+1}(\mathbf{x}, \mathbf{x}') = \exp\left(k_n(\mathbf{x}, \mathbf{x}') - 1\right) \qquad (\text{if } k_n(\mathbf{x}, \mathbf{x}) = 1) \tag{14}$$

Note that this result holds for any base kernel k_n, as long as $k_n(\mathbf{x}, \mathbf{x}) = 1$.

Infinitely deep kernels What happens when we apply this compsition many times, starting with the squared-exp kernel? In the infinite limit, this recursion converges to $k(x, y) = 1$ for all pairs of inputs. Figure 10 shows this kernel at different depths, including the degenerate limit.

One interpretation of why repeated feature transforms lead to this degenerate prior is that each layer can only lose information about the previous set of features. In the limit, the transformed features contain no information about the original input $\mathbf{x}$. Since the function doesn't depend on its input, it must be the same everywhere.

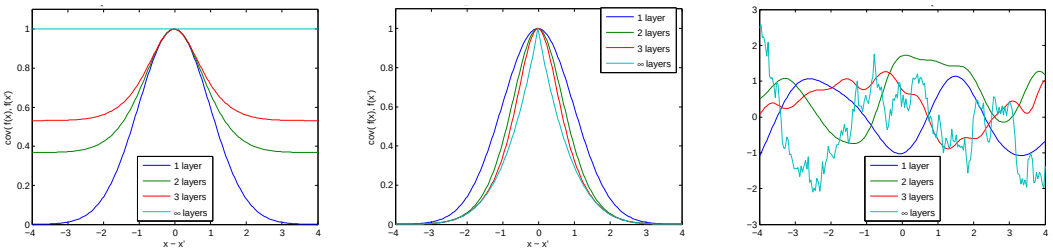

Iterated transform kernel | Connected transform kernel | Connected GP draws

Figure 10: Left: A kernel corresponding to composing features. In the limit, it becomes degenerate. Center: A non-degenerate version of the infinitely deep feature transform kernel. By connecting the inputs $\mathbf{x}$ to each layer, the function can still depend on its input even after arbitrarily many layers of computation. Right: Draws from this kernel.

A non-degenerate construction Again, following a suggestion from [9], we connect the inputs $\mathbf{x}$ to each layer. To do so, we simply augment the feature vector $\Phi_n(\mathbf{x})$ with the $\mathbf{x}$ at each layer:

$$k_{n+1}(\mathbf{x}, \mathbf{x}') = \exp\left(-\frac{1}{2}\left|\left|\begin{bmatrix}\Phi_n(\mathbf{x})\\ \mathbf{x}\end{bmatrix} - \begin{bmatrix}\Phi_n(\mathbf{x}')\\ \mathbf{x}'\end{bmatrix}\right|\right|_2^2\right) \tag{15}$$

$$k_{n+1}(\mathbf{x}, \mathbf{x}') = \exp\left(-\frac{1}{2}\sum_i \left[\phi_i(\mathbf{x}) - \phi_i(\mathbf{x}')\right]^2 - \frac{1}{2}||\mathbf{x} - \mathbf{x}'||_2^2\right) \tag{16}$$

$$k_{n+1}(\mathbf{x}, \mathbf{x}') = \exp\left(k_n(\mathbf{x}, \mathbf{x}') - 1 - \frac{1}{2}||\mathbf{x} - \mathbf{x}'||_2^2\right) \tag{17}$$

This kernel satisfies the recurrence $k - \log(k) = 1 + \frac{1}{2}||\mathbf{x} - \mathbf{x}'||_2^2$, a non-degenerate limit. The solution to this recurrence has no closed form, but it is continuous and differentiable everywhere except at $\mathbf{x} = \mathbf{x}'$. Samples from a GP with this prior are not differentiable, and locally resemble brownian motion, having a sort of fractal behavior.

6.1 Can "deep kernels" be useful models?

[2] showed that kernel machines, such as GPs, have limited generalization ability when they use a local kernel such as the squared-exp. However, many interesting non-local kernels can be constructed which allow non-trivial extrapolation, for example, periodic kernels. A periodic kernel can be viewed as a 2-layer-deep kernel, in which the first layer maps the input $x \to [\sin(x), \cos(x)]$, and the second layer maps through a set of radial-basis functions.

Kernels can capture many other types of generalization , such as translation and rotation invariance in images [6]. [15] even uses a deep neural network to learn feature transforms for kernels, which learn invariances in an unsupervised manner. In contrast, the relatively uninteresting properties of the kernels derived in this section suggest that deep computation is only powerful when it is combined with learning. For any specific problem, an arbitrary set of computations are unlikely to lead to useful generalization.

7 Related Work

Variational inference in deep Gausian processes was developed by [4], who also analyzed the effect of ARD in these models.

Several variants of deep models have been proposed, such as Bayesian Deep Networks [1] and Sum-product networks [11] These models also have no connections expect between adjacent layers, and perhaps may have similar pathologies as the number of layers increases.

Deep Density Networks [14] were constructed with invertibility in mind, with parameters encouraged to preserve information about lower layers.

[10] analyze the exploding-gradients problem in recurrent neural networks.

[8] note that performance of a MLP degrades as the number of layers with random weights increases.

8 Conclusions

- Deep GPs can be viewed as deep neural networks with a finite number of nonparametric hidden units.
- Deep GPs are analyzable using random matrix theory.
- Representations based on repeated composition of independently-initialized functions exhibit a pathology where the representation becomes invariant to all but one direction of variation.
- Connecting the input to each layer of a deep representation produces allows us to construct priors on deep functions without this pathology.

Acknowledgments

We thank Carl Rasmussen, Andrew McHutchon, Neil Lawrence, Andreas Diamanadou, James Lloyd, Creighton Heaukulani, Dan Roy and Mark van der Wilk for helpful discussions.

References

[1] Ryan P Adams, Hanna M Wallach, and Zoubin Ghahramani. Learning the structure of deep sparse graphical models. In *International Conference on Artificial Intelligence and Statistics*, pages 1–8, 2010.

[2] Yoshua Bengio, Olivier Delalleau, and Nicolas Le Roux. The curse of highly variable functions for local kernel machines. pages 107–114, 2006.

[3] Youngmin Cho. *Kernel methods for deep learning*. PhD thesis, University of California, San Diego, 2012.

[4] Andreas C Damianou and Neil D Lawrence. Deep gaussian processes. *arXiv preprint arXiv:1211.0358*, 2012.

[5] David Duvenaud, James Robert Lloyd, Roger Grosse, Joshua B. Tenenbaum, and Zoubin Ghahramani. Structure discovery in nonparametric regression through compositional kernel search. In *Proceedings of the 30th International Conference on Machine Learning*, June 2013.

[6] Imre Risi Kondor. *Group theoretical methods in machine learning*. 2008.

[7] James Martens. Deep learning via hessian-free optimization. In *Proceedings of the 27th International Conference on Machine Learning (ICML-10)*, pages 735–742, 2010.

[8] Grégoire Montavon, Dr Braun, Klaus-Robert Müller, et al. Layer-wise analysis of deep networks with gaussian kernels. *Advances in Neural Information Processing Systems (NIPS)*, 23: 1678–1686, 2010.

[9] Radford M Neal. *Bayesian learning for neural networks*. PhD thesis, University of Toronto, 1995.

[10] Razvan Pascanu, Tomas Mikolov, and Yoshua Bengio. Understanding the exploding gradient problem. *arXiv preprint arXiv:1211.5063*, 2012.

[11] Hoifung Poon and Pedro Domingos. Sum-product networks: A new deep architecture. In *Computer Vision Workshops (ICCV Workshops), 2011 IEEE International Conference on*, pages 689–690. IEEE, 2011.

[12] Salah Rifai, Grégoire Mesnil, Pascal Vincent, Xavier Muller, Yoshua Bengio, Yann Dauphin, and Xavier Glorot. Higher order contractive auto-encoder. In *Machine Learning and Knowledge Discovery in Databases*, pages 645–660. Springer, 2011.

[13] Salah Rifai, Pascal Vincent, Xavier Muller, Xavier Glorot, and Yoshua Bengio. Contractive auto-encoders: Explicit invariance during feature extraction. In *Proceedings of the 28th International Conference on Machine Learning (ICML-11)*, pages 833–840, 2011.

[14] Oren Rippel and Ryan Prescott Adams. High-dimensional probability estimation with deep density models. *arXiv preprint arXiv:1302.5125*, 2013.

[15] Ruslan Salakhutdinov and Geoffrey Hinton. Using deep belief nets to learn covariance kernels for Gaussian processes. In *Advances in Neural Information Processing Systems*, volume 20, 2008.

[16] Ercan Solak, Roderick Murray-Smith, E. Solak, William Leithead, Carl Rasmussen, and Douglas Leith. Derivative observations in gaussian process models of dynamic systems, 2003.

[17] Andrew G. Wilson and Ryan P. Adams. Gaussian process covariance kernels for pattern discovery and extrapolation. *arXiv: 1302.4245*, 2013.